



## Research article

## Simple synthesis of photoluminescent carbon dots from a marine polysaccharide found in shark cartilage

Kyung Woo Kim <sup>\*</sup>, Tae-Young Choi <sup>1</sup>, Yong Min Kwon, Jaon Young Hwan Kim

National Marine Biodiversity Institute of Korea, 75, Jangsan-ro 101beon-gil, Janghang-eup, Seocheon-gun, Chungcheongnam-do, 33662, Korea

## ARTICLE INFO

## Article history:

Received 18 February 2020

Accepted 14 July 2020

Available online 20 July 2020

## Keywords:

Carbon dots

Carbon quantum dots

Carbon-based luminescent nanomaterials

Hydrothermal treatment

Marine polysaccharide

Photoluminescent carbon dots

Shark cartilage

Zebrafish

## ABSTRACT

**Background:** For more than a decade, water-soluble, eco-friendly, biocompatible, and low-toxicity fluorescent nanomaterials have received considerable attention for their numerous *in vivo* and *in vitro* applications in biomedical imaging, disease diagnostics, and environmental monitoring. Owing to their tunable photoluminescence properties, carbon-based luminescent nanomaterials have shown great potential in bioimaging, photocatalysis, and biosensing among other applications.

**Results:** Marine environments provide excellent resources for the fabrication of these nanomaterials, because many marine organisms contain interesting trigger organic compounds that can be used as precursors. Herein, we synthesize multi-color emissive carbon dots (CDs) with an intrinsic photoluminescence quantum yield of 20.46%. These nanostructures were achieved through the one-step hydrothermal treatment of marine polysaccharide chondroitin sulfate, obtained from shark cartilage, in aqueous solution.

**Conclusions:** We successfully demonstrate the low toxicity of our marine resource-derived CDs in zebrafish, and provide an initial assessment of their possible use as a bioimaging agent. Notably, the newly synthesized CDs localize in the intestines of zebrafish larvae, thereby indicating their biocompatibility and potential use as *in vivo* dyes.

**How to cite:** Kim KW, Choi TY, Kwon YM, et al. Simple synthesis of photoluminescent carbon dots from a marine polysaccharide found in shark cartilage. *Electron J Biotechnol* 2020;47. <https://doi.org/10.1016/j.ejbt.2020.07.003>.

© 2020 Pontificia Universidad Católica de Valparaíso. Production and hosting by Elsevier B.V. All rights reserved. This is an open access article under the CC BY-NC-ND license (<http://creativecommons.org/licenses/by-nc-nd/4.0/>).

## 1. Introduction

Over the past decade, light-emitting quantum dots have been extensively applied in numerous fields, ranging from optoelectronics to biotechnology. However, some of them have applicability limitations: for instance, CdS-, CdSe-, and ZnS-based semiconductor or inorganic core-shell quantum dots exhibit serious toxicity and relatively low biocompatibility [1,2]. Alternatively, carbon-based luminescent nanomaterials, known as carbon-based quantum dots (carbon quantum dots (CQDs), graphene quantum dots (GQDs), and carbon dots (CDs or C-dots)) have emerged and attracted constant attention in many research areas, such as bioimaging, photocatalysis, electro- and biosensing, and medical diagnosis, owing to their tunable fluorescence

properties, low-cost fabrication, high biocompatibility, low toxicity, environmental friendliness, and excellent chemical stability and water solubility [1,3,4,5,6,7,8]. Particularly, CDs have optical properties that allow stepwise change of their emission from long- to short-wavelength; this is readily observed in a shift in the luminescence band in response to a displacement of the excitation wavelength. Synthetic approaches toward CDs involving both top-down and bottom-up processes have been proposed [9,10,11,12]. Top-down processes involve macroscopic graphite, soot, or activated charcoal as starting materials, transformed by chemical oxidation, arc discharge, or laser ablation [10,13]. Bottom-up processes involve the use of various molecular precursors such as citric acid, mono- or disaccharides, chitosan, or other organic raw materials that can be fabricated into CDs through thermal decomposition, microwave synthesis, hydrothermal treatment, or plasma treatment [6].

In recent years, various cost-effective and eco-friendly materials, terms as 'green precursors', have been introduced to fabricate luminescence carbon dots [14]. Table 1 shows the precursors, synthesizing approaches, and their optical properties. Most of them are fabricated by the hydrothermal treatment and emission colors are blue

\* Corresponding author.

E-mail address: [kimkw79@mabik.re.kr](mailto:kimkw79@mabik.re.kr) (K.W. Kim).

<sup>1</sup>Current address: Department of Pathology, Wonkwang University School of Medicine, 460, Iksan-daero, Iksan-si, Jeollabuk-do, 54538, Korea.

Peer review under responsibility of Pontificia Universidad Católica de Valparaíso.

**Table 1**  
Comparative investigation on luminescence properties of CDs fabricated by various green precursors.

Precursors	Synthetic method	Reaction conditions	Excitation wavelength (nm)	Emission color	Emission properties	Quantum yield (%)	Ref
Egg yolk	Plasma beam	120W, 3 min	302	Blue	Excitation dependent	5.96	[36]
Watermelon peels	Carbonization	220°C, 2 h	365	Blue	Excitation dependent	7.1	[29]
Gelatin	Hydrothermal	200°C, 3 h	350	Blue	Excitation dependent	31.6	[37]
Orange juice	Hydrothermal	120°C, 2 h 30 min	365	Green	Excitation dependent	26	[11]
Hair fibers	Hydrothermal	200°C, 24 h	365	Blue	Excitation dependent	10.75	[38]
Wine lees	Microwave-assisted pyrolysis	Unknown power, 18 bar, 1 h	366	Blue	Excitation dependent	6	[39]
Tofu wastewater	Heating	93°C, 3–5 h	410, 480	Blue, Green	Excitation dependent	54.49	[40]
Ginger	Hydrothermal	300°C, 2 h	365	Blue	Excitation dependent	13.4	[41]
Aloe	Hydrothermal	180°C, 11 h	365	Blue	Excitation dependent	10.37	[5]
Coriander leaves	Hydrothermal	240°C, 4 h	365	Green	Excitation dependent	6.48	[42]
Crab shells	Microwave-assisted pyrolysis	220°C, 10 min	370	Blue	Excitation dependent	12.86–19.84	[43]
Peach gum with ethylenediamine	Hydrothermal	180°C, 16 h	365	Blue	Excitation dependent	28.46	[44]
Onion waste with ethylenediamine	Hydrothermal	120°C, 2 h	360	Blue	Excitation dependent	28	[45]
<i>Trapa bispinosa</i> peel	Thermal oxidation	90°C, 2 h	365	Green	Excitation dependent	1.2	[46]
Cow manure	Chemical oxidation	120–300°C, 72 h	365	Green	Excitation dependent	65	[47]
Garlic( <i>Allium sativum</i> ) peel	Pyrolysis	315°C, 3 h	365	Green	Excitation dependent	12.4	[48]

or green depending on the excitation wavelength. They show stable fluorescent properties, good biocompatibility, low cytotoxicity and the possibilities of potential applications in many fields. In marine biotechnology, considerable research has been devoted to the synthesis of inorganic and organic nanomaterials, including CDs, from marine organisms: numerous marine-derived microbes, algae, spermatophytes, and animals including finfish and sponges are reported as possible sources [15]. All these living species contain several trigger compounds for the biosynthesis of nanoparticles, such as terpenoids, phenolics, pigments, alkaloids, and flavones. However, nanoparticle synthesis with marine resources has mostly been exploited for the preparation of metallic and semiconductor nanomaterials such as silver-, platinum-, and gold-containing nanostructures [15,16,17]. Among the plethora of marine-derived organic compounds, only chitin and its deacetylated derivative chitosan have so far been used as starting materials for the preparation of fluorescent CDs through hydrothermal and microwave treatment [9,18,19,20]. Chitosan is an abundant marine polysaccharide derived from chitin, which is extracted from the shells of sea arthropods including shrimps, crabs, and lobsters, and is a major promising raw material for applications in the biomedical industry. Chondroitin sulfate is also a marine polysaccharide derivative: it is a glycosaminoglycan (GAG) formed by repeating disaccharide units of glucuronic acid (GlcA) and *N*-acetylgalactosamine (GalNAc) [21,22]. Chondroitin sulfate is commonly extracted from the cartilage of terrestrial animals such as cattle, swine, and poultry. However, it can also be extracted and purified from the cartilage of marine organisms including sharks, squids, sturgeons, skates, and stingrays [23,24]. Interestingly, chondroitin sulfate from marine species is considered to be a better source owing to its finer sulfation pattern and improved safety than that derived from terrestrial animals [21].

Dietary supplements containing chondroitin sulfate are commonly used to treat or alleviate osteoarthritis [25], but other commercial applications have been increasingly explored owing to their good biocompatibility for biological tissue engineering, a field that focuses on the repair of bones, cartilage, and cutaneous wounds using synthetic tissues. Thus, biotechnology based on marine natural substances is believed to have significant potential and will possibly garner increasing interest toward industrial applications as research progresses.

In this regard, we demonstrate the simple synthesis of multicolor-photoluminescent CDs by using chondroitin sulfate from shark cartilage. Because shark cartilage is a major well-known marine resource to obtain chondroitin sulfate and easily obtained as a commercial product. The formation of CDs involves the hydrothermal carbonization of chondroitin sulfate in aqueous solution, an easy-to-

handle and green synthetic process. Furthermore, we show that these newly synthesized CDs are specifically detected in the intestines when they are administered to zebrafish larvae, thereby indicating their potential utilization as *in vivo* dyes.

## 2. Material and methods

### 2.1. Synthesis of chondroitin-sulfate-based CDs

Chondroitin sulfate sodium salt from shark cartilage was purchased from Sigma Aldrich (St. Louis, MO, USA). A total of 500 mg of chondroitin sulfate was dissolved in 20 mL of deionized water with vigorous stirring at ambient temperature. The faint yellowish mixture was transferred into a 25 mL polypropylene (PPL)-lined hydrothermal synthesis autoclave reactor (TEFIC biotech Co., Xi'an, China) and heated at 240°C for 3 h. The reactor was then cooled outside the furnace down to 25°C to yield a brown-colored solution.

Consequently, the supernatant was collected and filtered twice using 0.22 µm Minisart® NML syringe filters (Sartorius AG, Göttingen, Germany). Next, the solution was dialyzed against a Slide-A-Lyzer™ Dialysis cassette, 2 K MWCO cut-off (Thermo Scientific, Waltham, MA, USA) for 6 h at 27°C. Following dialysis, the CD-containing solution was mixed with chloroform at a volume ratio of 1:1 to remove unreacted or residual organic materials by liquid–liquid extraction. The upper layer was gathered and centrifuged at 50,000 rpm ( $r_{\max} = 214,000$  rcf,  $r_{\text{av}} = 155,000$  rcf,  $r_{\min} = 95,800$  rcf) for 15 min using an Optima XE-100 ultracentrifuge with a Type 90Ti fixed-angle rotor and 8.9 mL OptiSeal™ tubes to remove remaining residues (Beckman Coulter, Brea, CA, USA). The supernatant was then collected and stored in the dark at 4°C awaiting further use. The concentration of the obtained CDs was ~2.65 mg/mL.

### 2.2. Characterization of the CDs

Transmission electron microscopy (TEM) and energy dispersive X-ray spectroscopy (EDS) were performed on a JEM-ARM200F atomic resolution electron microscope with a cold field emission gun (cold FEG) operating at 200kV (JEOL, Tokyo, Japan). The particle sizes were analyzed using the Gatan Microscopy Suite® software (version 3.30; Pleasanton, CA, USA). Fluorescence spectroscopy and UV–vis spectrophotometry were both performed on a Molecular Devices SpectraMax i3x system (San Jose, CA, USA). The fluorescence spectra were measured using a 20 nm stepwise scan of the excitation wavelength between 350 nm and 510 nm. Fourier transform infrared (FT-IR) spectra were recorded on a JASCO FT-IR 4600 spectrometer

within the range of 400 to 4000  $\text{cm}^{-1}$  (Tokyo, Japan). The crystalline phase of the CDs was analyzed using a Bruker D8 ADVANCE X-ray diffractometer (Billerica, MA, USA). Fluorescence images of the CDs were captured by a Canon EOS M6 digital camera (Tokyo, Japan) under LED light and UV light at 430–440 nm and 365 nm of excitation wavelength, respectively.

### 2.3. Quantum yield measurements

The quantum yield ( $\Phi$ ) of the CDs was determined by comparing the fluorescence intensities and the absorbance values at 340 nm with those of a reference salt, quinine sulfate [11]. CD and quinine sulfate solutions, each with seven different concentrations, were prepared to calculate the quantum yield. Finally, the  $\Phi$  of the chondroitin-sulfate-based CDs was calculated using the following equation:

$$\Phi_{\text{CDs}} = \Phi_{\text{QS}} (m_{\text{CDs}}/m_{\text{QS}}) \left( \eta_{\text{CDs}}^2 / \eta_{\text{QS}}^2 \right) \quad (1)$$

where  $\Phi$  is the quantum yield,  $m$  is the slope of the integrated emission intensity, and  $\eta$  is the refractive index. The subscripts CDs and QS refer to the quantum dots and quinine sulfate, respectively. The reference quinine sulfate, with a well-known  $\Phi$  available from the literature ( $\Phi_{\text{QS}} = 0.54$ ) was dissolved in 0.1 M  $\text{H}_2\text{SO}_4$  ( $\eta_{\text{QS}} = 1.33$ ), while the CDs were suspended in deionized water ( $\eta_{\text{CDs}} = 1.33$ ) [11]. The absorbance spectra of these solutions were recorded at 340 nm; the fluorescence spectra were also measured at an excitation wavelength of 340 nm. We then plotted the collected integrated photoluminescence (PL) intensities of both quinine sulfate and the CDs against the respective absorbance values. For each curve, we determined the slope, which allowed for the calculation of  $\Phi$  of the CDs.

### 2.4. Zebrafish husbandry and CD treatment

Zebrafish embryos and adult zebrafish (*Danio rerio*) were raised and maintained under standard laboratory conditions according to a reported procedure [26]. Chondroitin sulfate-based CDs were administered to zebrafish larvae to determine if they could be detected in a specific organ. The cytotoxicity of the CDs was determined by exposing them to the larvae in a 6-well plate (10 larvae per well) in the dark at three concentrations: 25  $\mu\text{g}/\text{mL}$ , 50  $\mu\text{g}/\text{mL}$ , and 100  $\mu\text{g}/\text{mL}$ . To produce confocal microscope images, the zebrafish embryos was treated with the concentration of 100  $\mu\text{g}/\text{mL}$  and later observed with the microscope.

### 2.5. Image acquisition and processing

A Zeiss LSM800 confocal microscope (Jena, Germany) and a Nikon SMZ25 epi-fluorescence microscope (Tokyo, Japan) were used to obtain the optical images. Confocal stacks were analyzed using the

Zen Blue 2.1 software. All figures, labels, arrows, and scale bars were assembled or drawn using the Adobe Photoshop software.

## 3. Results and discussion

### 3.1. Optical properties of the CDs

The aqueous solution of CDs used for testing was obtained after hydrothermal treatment of chondroitin sulfate for 3 h and multiple purification steps, and had a clear yellowish-brown color to the naked eye in daylight. However, the color of the solution changed to yellowish-green and light blue under 430–440 nm and 365 nm of UV excitation, respectively (Fig. 1).

After that, the UV-vis absorption and PL emission depending on different excitation were examined to evaluate the optical properties of CD solutions. Fig. 2a and b displays the absorption and PL spectra of the as-obtained CDs. The UV-visible absorption spectrum presents a sharp peak at 287 nm and shoulder peak at about 324 nm, assigned to the  $\pi$ - $\pi^*$  transition of C=C bonds and the n- $\pi^*$  transition of the C=O bonds of the chondroitin scaffold, respectively (Fig. 2a) [27,28]. Additionally, the synthesized CDs revealed excitation-dependent emission characteristics. When the excitation wavelength was increased, the fluorescence intensity showed a steady decrease following an initial increase (Fig. 2b); however, the emission peak gradually red-shifted from 444 to 545 nm as the excitation wavelength went from 350 to 510 nm (Fig. 2c). This behavior demonstrates that the luminescence of the CDs depends on the surface states. Carbonization passivates the surface of the CDs, thereby introducing defects that entrap the generated excitons. This, in turn, induces unique, excitation-dependent luminescent phenomena through radiative recombination [11,19]. Finally, the photostability of the CDs was tested by exposing CD solution to 20  $\text{mW}/\text{cm}^2$  UV light under ambient air at dark room for different durations from 5 min to 360 min. As shown in Fig. 2d, the fluorescence intensity was decreased slightly until 60 min. However, the CDs still had maintained about 94% fluorescence intensity against the initial value with a prolonged exposure time of 360 min. It showed that as-obtained CDs from chondroitin sulfate hold good photostability.

### 3.2. Structural and compositional properties of CDs

The as-prepared CDs were characterized with FT-IR, TEM, XRD, and EDS to further analyze the structure of the CDs as well as their nature. FT-IR analysis showed the presence of functional groups attributable to the chondroitin scaffold on the surface of our CDs. The peaks at 1105  $\text{cm}^{-1}$ , 1262  $\text{cm}^{-1}$ , 1420  $\text{cm}^{-1}$ , 1671  $\text{cm}^{-1}$ , and 2963  $\text{cm}^{-1}$  were assigned to C—O—C (ether), (C=O)—OH (carboxylic acid), C=C (aromatic), (C=O)—NH<sub>2</sub> (amide), and C—H, respectively (Fig. S1). We expected that the slightly or highly hydrophilic groups of C—O—C, (C=O)—O, and (C=O)—NH<sub>2</sub> were able to stabilize the CDs

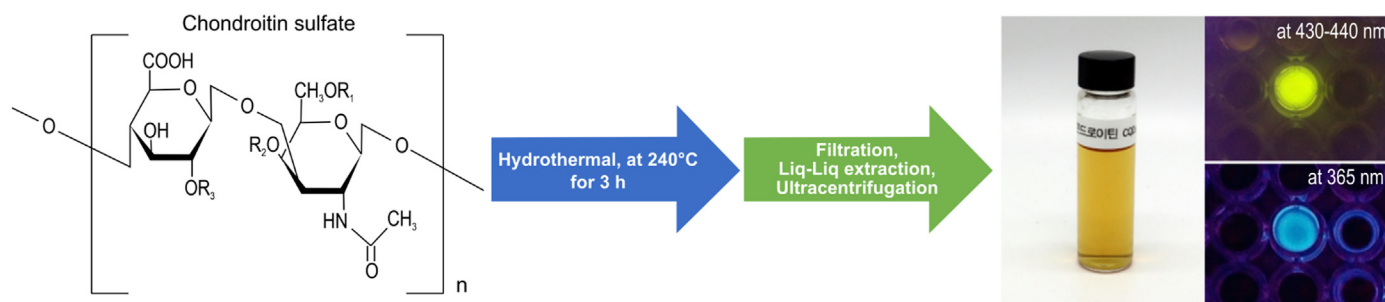


**Fig. 1.** Experimental scheme illustrating the fabrication process of CDs from chondroitin sulfate through hydrothermal treatment, and optical images of the obtained CDs: the clear yellowish-brown color can be observed for the solution under visible light, the green fluorescence emission is observed under 430–440 nm of LED light, and the light blue fluorescence emission under 365 nm of UV excitation;

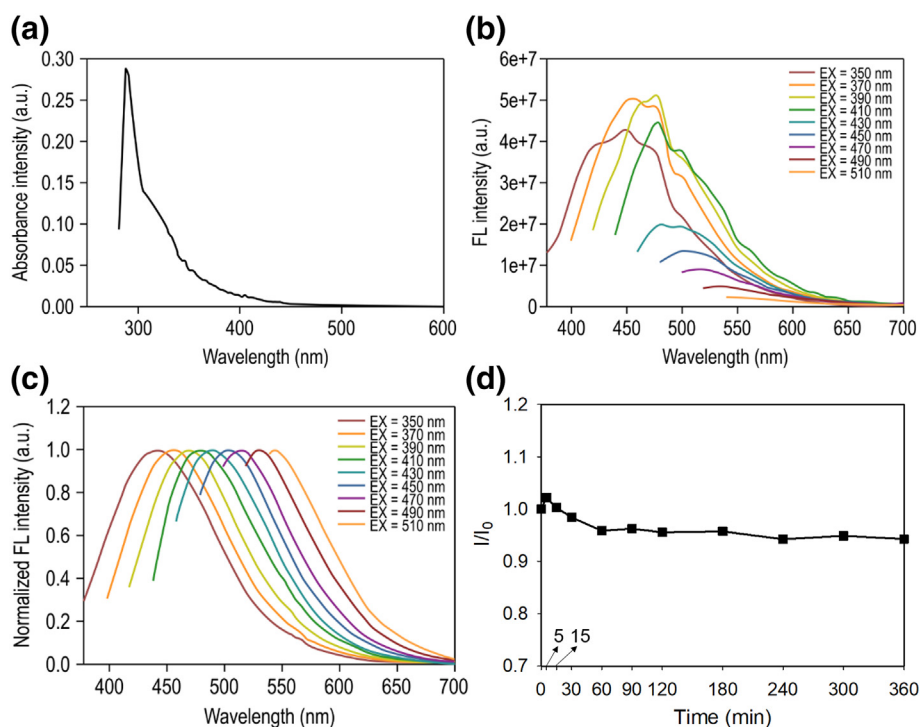


**Fig. 2.** (a) UV-vis absorption spectra of CDs; (b) PL emission spectra measured by progressively longer excitation wavelengths with 20 nm increments from 350 nm to 510 nm; (c) Normalized PL emission spectra that show a red-shift with increasing excitation wavelength; (d) Evaluation of the photostability under UV exposure during different time intervals.

in aqueous solution. Actually, the fabricated CDs have been still dispersed well in deionized water at 4°C for 280 days without any precipitation. Moreover, the functional groups on the surface of the

CDs also affect the luminescence characteristics [29]. TEM images revealed that the CDs were spherical and polydispersed (Fig. 3a). Particle size analysis showed a broad size distribution between 19.6 and ~60 nm. Fig. 3b shows the particle size distribution of the CDs: most of the particles were approximately 50 nm in size. Interestingly, our chondroitin sulfate-derived CDs have a larger diameter, mainly >20 nm, compared to that of typical CDs (mostly <10 nm) [12]. However, bigger CDs have recently been reported, synthesized by controlling the type or initial concentration of the precursor and selecting specific fabrication techniques [30,31,32,33]. The size of carbon dots seems to concern its crystallized nature. If the carbon dots with highly crystallization, the size is usually evaluated to be around 10 nm or less. On the contrary, the size range of carbon dots with sole amorphous or mixed with crystallized structure is much larger than usual one of below 10 nm [11,34].

To further confirm the crystalline nature of our CDs, we recorded an XRD spectrum, presented in Fig. 4a. A peak attributable to the [002] plane appeared broadly at 23.4°, which allowed us to calculate the corresponding interlayer spacing in the CDs using Bragg's equation ( $2d\sin\theta = n\lambda$ ). We calculated an interlayer spacing of 0.379 nm for the [002] plane, which is slightly larger than that of graphite, calculated at 0.34 nm. This could be attributed to an increase in the amorphous carbon phase due to the presence of oxygen-containing groups [11,35]. From the result, we assumed that the CD solution was mixed with more amorphous and less crystallized structures. In addition, we obtained the elemental distributions on the surface of the CDs by EDS (Fig. S2). The EDS data confirmed that most of the surface consisted of carbon and oxygen. Traces of sodium (Na) and sulfur (S) were also detected due to the 10% impurities present in commercial chondroitin sulfate that we used as our starting material.

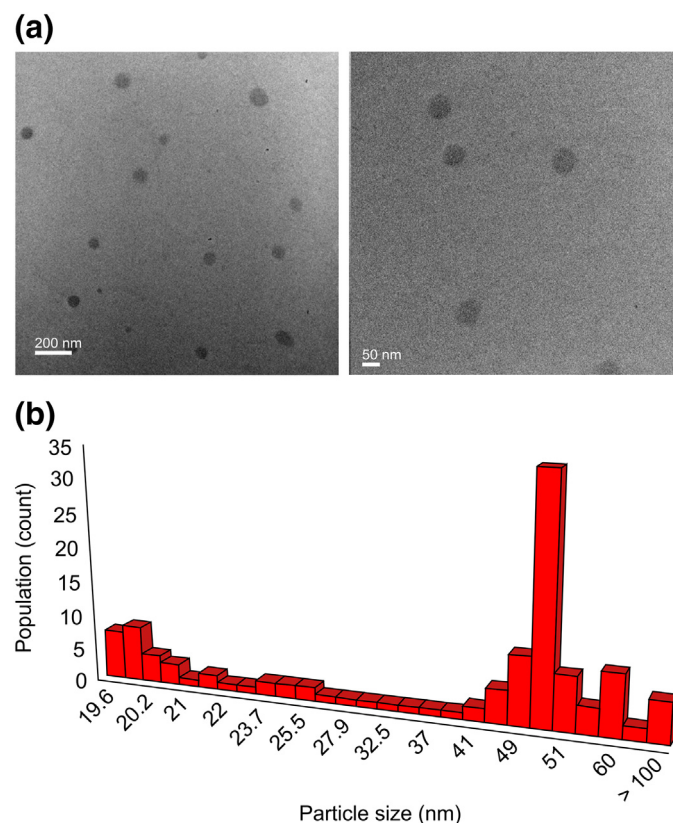


**Fig. 3.** (a) TEM image of CDs from chondroitin sulfate and (b) histogram of the size distribution of the synthesized CDs analyzed by the Gatan Microscopy Suite® software.

### 3.3. Quantum yield of the CDs

The PL quantum yield (PLQY) involved with the brightness and signal intensity of the fluorescence is the most important parameter in the verification of the characteristic property of photoluminescence species.

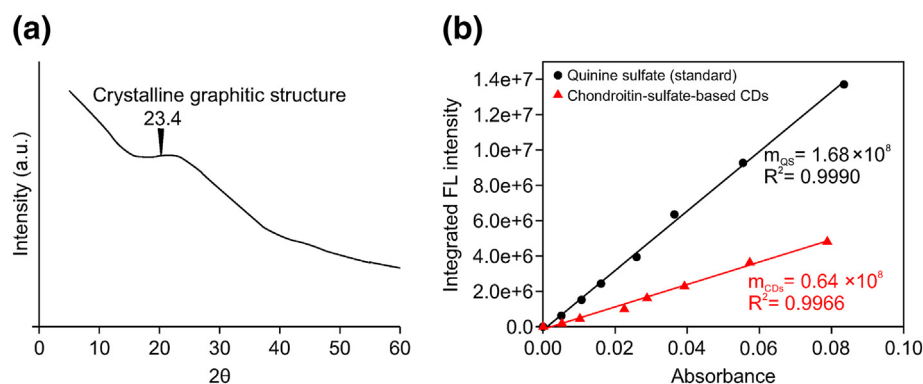


**Fig. 4.** (a) XRD profiles of CDs evidencing a [002] plane diffraction peak at 23.4° and (b) linear regression plots of fluorescence (FL) intensity vs. absorbance of CDs and quinine sulfate.

The quantum yield can be measured using the absolute method or the relative method, with the latter being utilized to calculate the quantum yield of CDs in this paper. Because the relative method is the easiest way to determine the PLQY were introduced by comparing luminescent intensities of the sample with the standard compound. To calculate the quantum yield, the quinine sulfate solutions were prepared in 0.1 M  $H_2SO_4$  at various concentrations as reference. The fluorescence intensities and absorbance values were then measured at 340 nm for both reference samples and synthesized CDs. The obtained data on quinine sulfate and CDs were plotted and fitted by linear regression (Fig. 4b). Based on the slopes of the linear regression fit, the quantum yield of CDs from chondroitin sulfate was then determined to be 20.46%. Compared to the quantum yields of other carbon-based quantum dots obtained from a variety of other precursors with hydrothermal treatment, the marine-synthesized CDs achieved a reasonable inherent quantum yield without further surface modification [4].

### 3.4. *In vivo* images after treating zebrafish larvae with CDs

Zebrafish is an already well-known model organism to investigate the nature and roles of specific genes as well as their signaling pathways in developmental owing to its near transparency and efficient breeding rate (hundreds of offspring at weekly intervals). For that reason, zebrafish has been extensively used in biological, biochemical, and medical research. Recently, the toxicity, biocompatibility, and *in vivo* transportation of nanoparticles or drugs are often investigated by using zebrafish [10]. To verify the toxicity and *in vivo* imaging assessment of the CDs, we utilized zebrafish larvae. We first treated the zebrafish larvae with CDs, starting three days post fertilization (dpf), for 24 h in the dark after determining the maximum tolerated concentration without cytotoxicity (data not shown). After the CD treatment at 4 dpf with the highest concentration of 100  $\mu g/mL$  that showed no cytotoxicity at

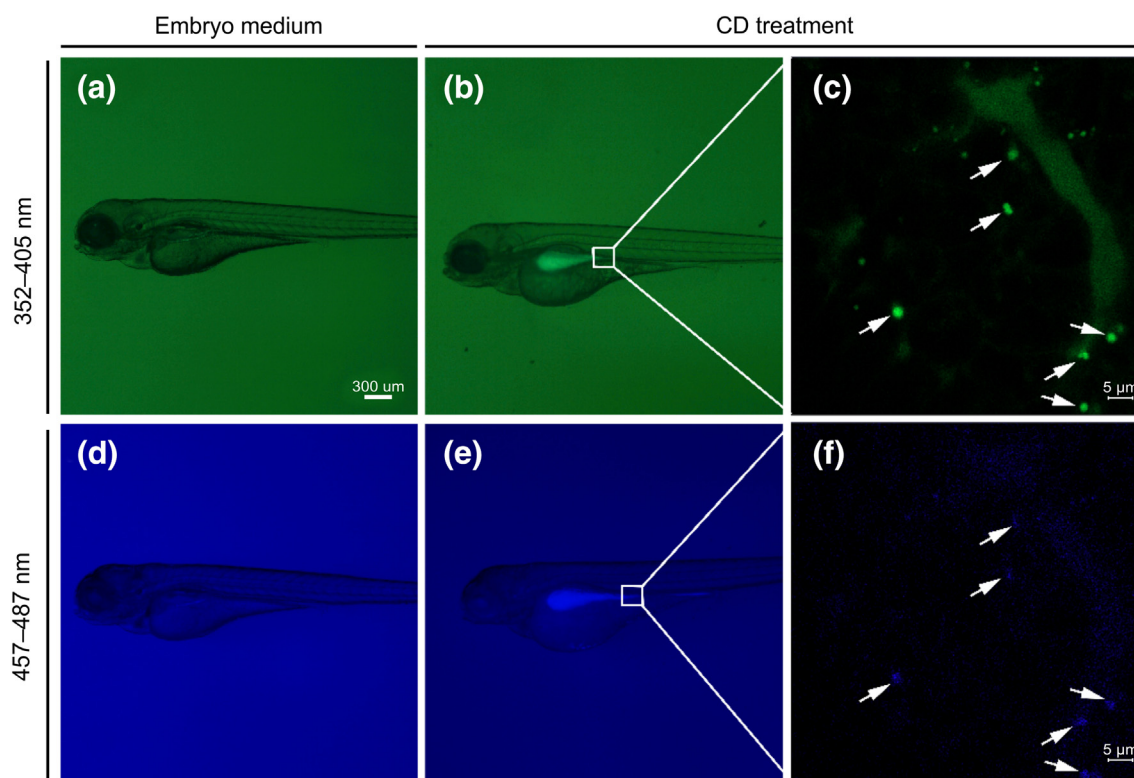


**Fig. 5.** Administering CDs to zebrafish larvae results in fluorescent imaging in the intestine. (b) Green and (e) light-blue fluorescence were detected by treating the zebrafish larvae with CDs for 24 h from 4 dpf compared to non-treated larvae (a), (d). Confocal images showing CDs-treated zebrafish larvae reveal the specific accumulation of fluorescence as indicated by arrows ((c), (f)).

pretreatment, green and blue fluorescence emissions were detected in the intestine of the treated larvae (Fig. 5b and e) whereas non-treated larvae displayed no fluorescence (Fig. 5a and d). The fluorescence intensity was highest in the intestines of the zebrafish larvae, with specific regions of the intestines displaying a differential accumulation of CDs (Fig. 5c and f). Based on the aforementioned results, we established that our water-soluble CDs can readily enter and accumulate inside the body of zebrafish and confirmed our hypothesis that the fabricated CDs can be of potential use for clinical applications as fluorescent probes with low toxicity.

#### 4. Conclusions

In conclusion, we have developed a simple one-step synthetic method for the preparation of functional materials from chondroitin sulfate derived from shark cartilage: multicolor PL CDs. These CDs showed good PL properties without any additional chemical modification. Furthermore, when zebrafish larvae were treated with CDs, green and blue fluorescence could be selectively detected in the intestines. The localization of the CDs in the intestines may indicate that CDs can potentially bind to specific target molecules such as lipid droplets. Further study is required to confirm this suggestion, and to explore the binding partner of CDs in the intestines of zebrafish larvae to exploit this *in vivo* imaging method. CDs are incredibly versatile materials, because their optical properties make them potentially applicable in a wide variety of research and industrial fields; hence, we expect that these novel marine-derived CDs would be of high value for both fundamental research and industrial applications, including marine biotechnology, in the near future.

#### Conflict of interest

The authors declare that they have no conflict of interest.

#### Financial support

This work was supported by the National Marine Biodiversity Institute of Korea (MABIK) [grant number 2020M00600].

#### Acknowledgments

We would like to thank Editage ([www.editage.com](http://www.editage.com)) for English language editing.

#### Supplementary material

<https://doi.org/10.1016/j.ejbt.2020.07.003>

#### References

- Chan KK, Yap SHK, Yong KT. Biogreen synthesis of carbon dots for biotechnology and nanomedicine applications. *Nano-Micro Lett.* 2018;10:72. <https://doi.org/10.1007/s40820-018-0223-3>.
- Matea CT, Mocan T, Tabaran F, et al. Quantum dots in imaging, drug delivery and sensor applications. *Int J Nanomedicine.* 2017;12:5421–31. <https://doi.org/10.2147/IJN.S138624>.
- Dong Y, Wang R, Li G, et al. Polyamine-functionalized carbon quantum dots as fluorescent probes for selective and sensitive detection of copper ions. *Anal Chem.* 2012;84:6220–4. <https://doi.org/10.1021/ac3012126>.
- Lim SY, Shen W, Gao Z. Carbon quantum dots and their applications. *Chem Soc Rev.* 2015;44:362–81. <https://doi.org/10.1039/c4cs00269e>.
- Xu H, Yang X, Li G, et al. Green synthesis of fluorescent carbon dots for selective detection of tartrazine in food samples. *J Agric Food Chem.* 2015;63:6707–14. <https://doi.org/10.1021/acs.jafc.5b02319>.
- Wang R, Lu KQ, Tang ZR, et al. Recent progress in carbon quantum dots: Synthesis, properties and applications in photocatalysis. *J Mater Chem A.* 2017;5:3717–34. <https://doi.org/10.1039/c6ta08660h>.
- Das P, Ganguly S, Mondal S, et al. Heteroatom doped photoluminescent carbon dots for sensitive detection of acetone in human fluids. *Sens Actuators B Chem.* 2018;266:583–93. <https://doi.org/10.1016/j.snb.2018.03.183>.
- Das P, Ganguly S, Banerjee S, et al. Graphene based emergent nanolights: A short review on the synthesis, properties and application. *Res Chem Intermediat.* 2019;45:3823–53. <https://doi.org/10.1007/s11164-019-03823-2>.
- Liu X, Pang J, Xu F, et al. Simple approach to synthesize amino-functionalized carbon dots by carbonization of chitosan. *Sci Rep.* 2016;6:31100. <https://doi.org/10.1038/srep31100>.
- Kang YF, Li YH, Fang YW, et al. Carbon quantum dots for zebrafish fluorescence imaging. *Sci Rep.* 2015;5:11835. <https://doi.org/10.1038/srep11835>.
- Sahu S, Behera B, Maiti TK, et al. Simple one-step synthesis of highly luminescent carbon dots from orange juice: Application as excellent bio-imaging agents. *Chem Commun.* 2012;48:8835–7. <https://doi.org/10.1039/c2cc33796g>.
- Das R, Bandyopadhyay R, Pramanik P. Carbon quantum dots from natural resource: A review. *Mater Today Chem.* 2018;8:96–109. <https://doi.org/10.1016/j.mtchem.2018.03.003>.
- Farshbaf M, Davaran S, Rahimi F, et al. Carbon quantum dots: Recent progresses on synthesis, surface modification and applications. *Artif Cells Nanomed Biotechnol.* 2018;46:1331–48. <https://doi.org/10.1080/21691401.2017.1377725>.
- Ganguly S, Das P, Banerjee S, et al. Advancement in science and technology of carbon dot-polymer hybrid composites: A review. *Funct Compos Struct.* 2019;1:022001. <https://doi.org/10.1088/2631-6331/ab0c80>.
- Asmathunisha N, Kathiresan K. A review on biosynthesis of nanoparticles by marine organisms. *Colloids Surf B Biointerfaces.* 2013;103:283–7. <https://doi.org/10.1016/j.colsurfb.2012.10.030>.
- Chinnappan RS, Kandasamy K, Sekar A. A review on marine based nanoparticles and their potential applications. *Afr J Biotechnol.* 2015;14:1525–32. <https://doi.org/10.5897/ajb2015.14527>.
- Patil MP, Kim G-D. Marine microorganisms for synthesis of metallic nanoparticles and their biomedical applications. *Colloids Surf B Biointerfaces.* 2018;172:487–95. <https://doi.org/10.1016/j.colsurfb.2018.09.007>.
- Janus Ł, Piatkowski M, Radwan-Pragłowska J, et al. Chitosan-based carbon quantum dots for biomedical applications: Synthesis and characterization. *Nanomaterials.* 2019;9:274. <https://doi.org/10.3390/nano9020274>.
- Yang Y, Cui J, Zheng M, et al. One-step synthesis of amino-functionalized fluorescent carbon nanoparticles by hydrothermal carbonization of chitosan. *Chem Commun.* 2012;48:380–2. <https://doi.org/10.1039/c1cc15678k>.
- Shchipunov YA, Khlebnikov ON, Silant'ev VE. Carbon quantum dots hydrothermally synthesized from chitin. *Polym Sci Ser B.* 2015;57:16–22. <https://doi.org/10.1134/S1560090415010121>.
- Vázquez JA, Rodríguez-Amado I, Montemayor MI, et al. Chondroitin sulfate, hyaluronic acid and chitin/chitosan production using marine waste sources: Characteristics, applications and eco-friendly processes: A review. *Mar Drugs.* 2013;11:747–74. <https://doi.org/10.3390/md11030747>.
- Volpi N. Chondroitin sulfate safety and quality. *Molecules.* 2019;24:1447. <https://doi.org/10.3390/molecules24081447>.
- Maccari F, Galeotti F, Volpi N. Isolation and structural characterization of chondroitin sulfate from bony fishes. *Carbohydr Polym.* 2015;129:143–7. <https://doi.org/10.1016/j.carbpol.2015.04.059>.
- Mazlan MSA, Ichwan SJA, Rosli N. Effects of chondroitin sulfate (CS) on (HeLa) cervical cancer and breast cancer (MCF-7) cell lines. *J Int Dent Med Res.* 2019;12:38–41. <http://iirep.iium.edu.my/id/eprint/71833>.
- Henrotin Y, Mathy M, Sanchez C, et al. Chondroitin sulfate in the treatment of osteoarthritis: From *in vitro* studies to clinical recommendations. *Ther Adv Musculoskelet Dis.* 2010;2:335–48. <https://doi.org/10.1177/1759720X10383076>.
- Westerfield M. The zebrafish book: A guide for the laboratory use of zebrafish (*Danio rerio*). 4th ed. Eugene: University of Oregon Press; 2000.
- Atabaev TS. Doped carbon dots for sensing and bioimaging applications: A minireview. *Nanomaterials.* 2018;8:342. <https://doi.org/10.3390/nano8050342>.
- Das P, Maity PP, Ganguly S, et al. Biocompatible carbon dots derived from κ-carrageenan and phenyl boronic acid for dual modality sensing platform of sugar and its anti-diabetic drug release behavior. *Int J Biol Macromol.* 2019;132:316–29. <https://doi.org/10.1016/j.ijbiomac.2019.03.224>.
- Zhou J, Sheng Z, Han H, et al. Facile synthesis of fluorescent carbon dots using watermelon peel as a carbon source. *Mater Lett.* 2012;66:222–4. <https://doi.org/10.1016/j.matlet.2011.08.081>.
- Chen L, Zhang J. Carbon dots with tunable photoluminescence properties. Proceedings of the 2nd International Conference of Theoretical and Applied Nanoscience and Nanotechnology: 2018 June 10–12. Niagara Falls: Canada Avestia Publishing; 2018. <https://doi.org/10.11159/tann18.129>.
- Papaioannou N, Titirici MM, Sapekin A. Investigating the effect of reaction time on carbon dot formation, structure, and optical properties. *ACS Omega.* 2019;4:21658–65. <https://doi.org/10.1021/acsomega.9b01798>.
- Yahyazadeh E, Shemirani F. Easily synthesized carbon dots for determination of mercury(II) in water samples. *Heliyon.* 2019;5:e01596. <https://doi.org/10.1016/j.heliyon.2019.e01596>.
- Hoan BT, Tam PD, Pham VH. Green synthesis of highly luminescent carbon quantum dots from lemon juice. *J Nanotechnol.* 2019;2019:1–9. <https://doi.org/10.1155/2019/2852816>.
- Liu W, Sun X, Pan W, et al. Highly crystalline carbon dots from fresh tomato: UV emission and quantum confinement. *Nanotechnology.* 2017;28:485705. <https://doi.org/10.1088/1361-6528/aa900b>.
- Peng J, Gao W, Gupta BK, et al. Graphene quantum dots derived from carbon fibers. *Nano Lett.* 2012;12:844–9. <https://doi.org/10.1021/nl2038979>.

- [36] Wang J, Wang CF, Chen S. Amphiphilic egg-derived carbon dots: Rapid plasma fabrication, pyrolysis process, and multicolor printing patterns. *Angew Chem Int Ed*. 2012;51:9297–301. <https://doi.org/10.1002/anie.201204381>.
- [37] Liang Q, Ma W, Shi Y, et al. Easy synthesis of highly fluorescent carbon quantum dots from gelatin and their luminescent properties and applications. *Carbon N Y*. 2013;60:421–8. <https://doi.org/10.1016/j.carbon.2013.04.055>.
- [38] Guo Y, Zhang L, Cao F, et al. Thermal treatment of hair for the synthesis of sustainable carbon quantum dots and the applications for sensing  $Hg^{2+}$ . *Sci Rep*. 2016;6:35795. <https://doi.org/10.1038/srep35795>.
- [39] Varisco M, Zufferey D, Ruggi A, et al. Synthesis of hydrophilic and hydrophobic carbon quantum dots from waste of wine fermentation. *R Soc Open Sci*. 2017;4:170900. <https://doi.org/10.1098/rsos.170900>.
- [40] Zhang J, Wang H, Xiao Y, et al. A simple approach for synthesizing of fluorescent carbon quantum dots from tofu wastewater. *Nanoscale Res Lett*. 2017;12:611. <https://doi.org/10.1186/s11671-017-2369-1>.
- [41] Li C-L, Ou C-M, Huang C-C, et al. Carbon dots prepared from ginger exhibiting efficient inhibition of human hepatocellular carcinoma cells. *J Mater Chem B*. 2014;2:4564–71. <https://doi.org/10.1039/c4tb00216d>.
- [42] Sachdev A, Gopinath P. Green synthesis of multifunctional carbon dots from coriander leaves and their potential application as antioxidants, sensors and bioimaging agents. *Analyst*. 2015;140:4260–9. <https://doi.org/10.1039/c5an00454c>.
- [43] Yao Y-Y, Gedda G, Girma WM, et al. Magnetofluorescent carbon dots derived from crab shell for targeted dual-modality bioimaging and drug delivery. *ACS Appl Mater Interfaces*. 2017;9:13887–99. <https://doi.org/10.1021/acsami.7b01599>.
- [44] Liao J, Cheng Z, Zhou L. Nitrogen-doping enhanced fluorescent carbon dots: Green synthesis and their applications for bioimaging and label-free detection of  $Au^{3+}$  ions. *ACS Sustain Chem Eng*. 2016;4:3053–61. <https://doi.org/10.1021/acssuschemeng.6b00018>.
- [45] Bandi R, Gangapuram BR, Dadigala R, et al. Facile and green synthesis of fluorescent carbon dots from onion waste and their potential applications as sensor and multicolour imaging agents. *RSC Adv*. 2016;6:28633–9. <https://doi.org/10.1039/c6ra01669c4mm>.
- [46] Mewada A, Pandey S, Shinde S, et al. Green synthesis of biocompatible carbon dots using aqueous extract of *Trapa bispinosa* peel. *Mater Sci Eng C*. 2013;33:2914–7. <https://doi.org/10.1016/j.msec.2013.03.018>.
- [47] D'Angelis do ES Barbosa Cintya, Corrêa JR, Medeiros GA, et al. Carbon dots (C-dots) from cow manure with impressive subcellular selectivity tuned by simple chemical modification. *Chem A Eur J*. 2015;21:5055–60. <https://doi.org/10.1002/chem.201406330>.
- [48] Das P, Ganguly S, Maity PP, et al. Converting waste *Allium sativum* peel to nitrogen and Sulphur co-doped photoluminescence carbon dots for solar conversion, cell labeling, and photobleaching diligences: A path from discarded waste to value-added products. *J Photochem Photobiol B*. 2019;197:111545. <https://doi.org/10.1016/j.jphotobiol.2019.111545>.